



ELSEVIER

Journal of Nuclear Materials 266–269 (1999) 370–375

journal of  
nuclear  
materials

# Recombination and ion loss in C-Mod detached divertor discharges

B. Lipschultz<sup>\*</sup>, J.L. Terry, C. Boswell, S.I. Krasheninnikov, B. LaBombard, D.A. Pappas

Massachusetts Institute of Technology, Plasma Science and Fusion Center, Room NW 17-103, 77 Massachusetts Avenue, Cambridge, MA 02139, USA

## Abstract

We present detailed profiles of the magnitude and location of volumetric recombination occurring in the Alcator C-Mod divertor region during detached divertor discharges. The recombination sink (for ions) is compared to the ion current collected at the divertor plates both as a function of location on the plate and across the entire divertor. We find that, depending on plasma conditions, volume recombination can account for the removal of 10–75% of the ions flowing on detached flux surfaces. A similarly important cause of the observed ion current loss appears to be the reduction in divertor ion sources upstream from the plate. Changes in the ion source rate are consistent with changes in power flowing from the SOL into the divertor region. The lowest levels of recombination are found in H-mode discharges where detachment is induced through puffing of N<sub>2</sub> gas. In these cases the observed ion current loss is due almost entirely to decrease in the ion source. This shows that recombination is not a necessary condition for detachment. © 1999 Elsevier Science B.V. All rights reserved.

*Keywords:* Recombination; Divertor spectroscopy; Detached plasma; Alcator C-Mod

## 1. Introduction

Divertor detachment is characterized by significant decreases in measured ion and heat flux as well as plasma pressure at the divertor plate (e.g. Refs. [1–3]). The general experimental features of divertor detachment have been fairly well characterized [3–6]. Most important among these are reductions in plasma pressure and heat flux at the divertor plate relative to attached (or upstream) values. These essential features explain the attraction of this type of operation. When power flows out of the core plasma, it is dispersed through radiation to the walls rather than being conducted into a relatively smaller area on the divertor plates.

It has been predicted that volume recombination provides the mechanism for this current loss [7–12].

Recombination has been experimentally shown to exist in the divertor [13–16] and its magnitude is significant [13,16]. In this paper we present detailed profiles of the recombination magnitude and location. We find that the measured levels of recombination sink cannot explain all of the ion current loss. We infer that the remaining loss in ion current is due to a drop in ion source rate further upstream in the divertor. This limitation in ion source rate appears to be due to limitations in power flow into the ionizing region.

## 2. Experiment and technique

The measurements presented here are from the Alcator C-Mod tokamak. Basic characteristics of the experiment and diagnostics are described elsewhere [17]. The data used in this study were acquired with 5.3 T toroidal field at the plasma center and plasma currents in the range 0.8–1.0 mA. All discharges were diverted with a single field null at the bottom of the machine,

<sup>\*</sup> Corresponding author. Tel.: +1-617 253 8636; fax: +1-617 253 0627; e-mail: blip@psfc.mit.edu.

Fig. 1. Included in this study are data from ohmically heated as well as ICRF-heated discharges (both L- and H-mode).

The primary diagnostics used for this study were a visible spectrometer and Langmuir probes located on the surface of the divertor plates. The visible spectrometer is an  $f/4$ , 0.25 m focal length system. Up to 16 fiber inputs, corresponding to different chords within the views O and T of the plasma shown in Fig. 1, can be monitored simultaneously. The spectrometer has a wavelength resolution of 1.5–2.5 nm for these data and a temporal resolution of 56 ms. It is employed to measure the  $D^0$  Balmer spectrum of transitions  $p \rightarrow 2$  ( $p=5$  through 11). The Langmuir probes are described in detail elsewhere [18]. The analysis of probe data provides the profiles of  $n_e$ ,  $T_e$ , and ion current over the surface of the divertor plates.

We have analyzed Balmer series spectral emission to determine the characteristics of the plasma near the divertor surface. Such characteristics are an average over any recombining region within the viewing chord. The Balmer lines are significantly broadened compared to the instrumental width. We fit a Voigt profile to these line shapes to obtain the FWHM of the  $p=6,7,8,9 \rightarrow 2$  lines. Using standard Stark analysis techniques (e.g. Ref. [19]), we obtain the density with typical uncertainties of  $2\text{--}3 \times 10^{20} \text{ m}^{-3}$ .

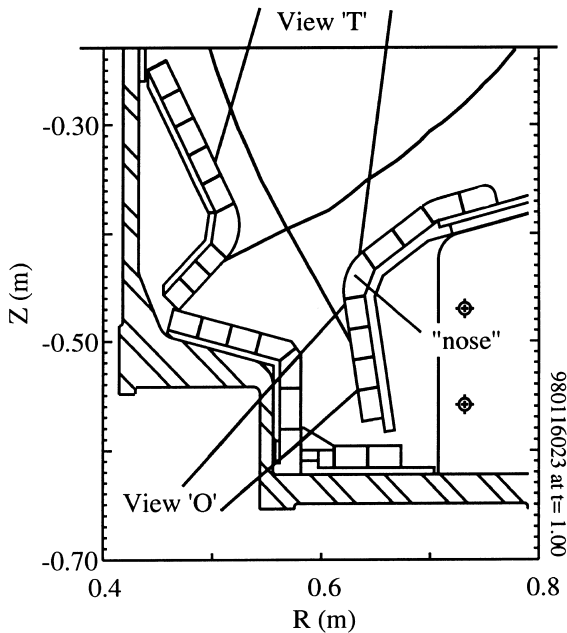


Fig. 1. The Alcator C-Mod divertor region. View O includes seven chordal views of the outer divertor. View T includes eight chordal views of both divertors. The emission pattern shown is from an inverted CCD image filtered for  $D_\gamma$  from a detached divertor discharge.

We also estimate the electron temperature from the intensities of the Balmer spectrum. The population densities of excited states, determined through their corresponding emission intensities, are dominated by recombination [16] and should scale according to the Saha–Boltzmann distribution. We perform a least-squares fit of the population densities:

$$n_p \propto \frac{p^2}{T_e^{3/2}} \exp\left(\frac{13.605}{T_e p^2}\right). \quad (1)$$

where  $(13.605/p^2)$  is the ionization energy for the  $p^{\text{th}}$  level. Due to the overlap of the  $p=9$  and  $10 \rightarrow 2$  lines as well as their large ‘wings’, which are difficult to fit, we have only included the  $p=5$  through  $8 \rightarrow 2$  lines in this  $T_e$  analysis. The inferred  $T_e$ s are found to be in the range from 0.4 to 0.8 eV. The uncertainties of this measurement are related to the possible modification of population densities by the opacity of the plasma to  $Ly_{\alpha,\beta}$  or by excitation from the ground state. Our estimate of the  $T_e$  uncertainty is  $\sim \pm 0.1$  eV.

If the viewed plasma is opaque to Lyman series radiation, the local recombination and ionization rates are strongly affected. By measuring  $Ly_\beta$  and  $D_\alpha$  intensities along the same line-of-sight through a recombining region, we have found [16] that up to 50% of the  $Ly_\beta$  photons are trapped and lost before reaching the spectrometer. This implies even stronger trapping ( $\geq 95\%$ ) of  $Ly_\alpha$  emission. The modeling [16] of the effect of such  $Ly_{\alpha,\beta}$  trapping on the recombination rate shows that at these levels of trapping the recombination rate is reduced by a factor  $\sim 5$ . This determination is currently being refined using a code which models the radiation transfer. (See the paper by Terry [20] in this journal issue.) Because the VUV spectrometer used for the characterization of plasma opacity is not available at all times and has a limited set of views (the inner divertor), we have assumed that the plasma opacity is the same in all divertor recombination regions.

The primary method used in estimating the volume recombination rate is based on previous work in which a collisional radiative model has been used to interpret the measured intensities (Ref. [16] and references therein). A factor  $R$ , ‘recombinations per photon’, is defined and calculated which allows determination of the recombination rate, given the knowledge of the emitting region  $n_e$ ,  $T_e$ ,  $D^0$  line brightness, and opacity to the Lyman series. We have not included the effects of radiation transport in wavelength and space which, as mentioned above, is the subject of current study [20]. We have applied this formalism to the spatially resolved emission lines of  $D_\gamma$  using the locally measured  $n_e$ ,  $T_e$ , and the assumed opacity.

In previous studies [13,16,21] we have relied on an assumed  $T_e \sim 1.0$  eV to estimate the recombinations per

photon factor for all locations. This was based on the analysis of spectra from a region of limited extent at the inner divertor plate. In this current study the effect of both the local  $T_e$  and  $n_e$  have been taken into account. Because  $T_e$  is lower than previously assumed, the recombinations per photon factors has increased substantially ( $\sim \times 5$ ) over that for 1.0 eV.

### 3. Expansion of the recombination region

The location of volume recombination is important for understanding its development and its effects on the plasma. The initial growth of the recombination region at the outer divertor plate as detachment starts is shown in Fig. 2(a)–(c). These data are from view O shown in Fig. 1, where the viewing chords are almost perpendicular to the plate surface. The separatrix strike point is indicated by  $z=0$ . The outer divertor ‘nose’ is at  $z \sim 5$  cm. Each chord provides spatially resolved information (in  $z$ ) about the recombination and is an integral through the divertor fan (Fig. 1). Even in the initial time frame shown (0.55 s), before any observable pressure

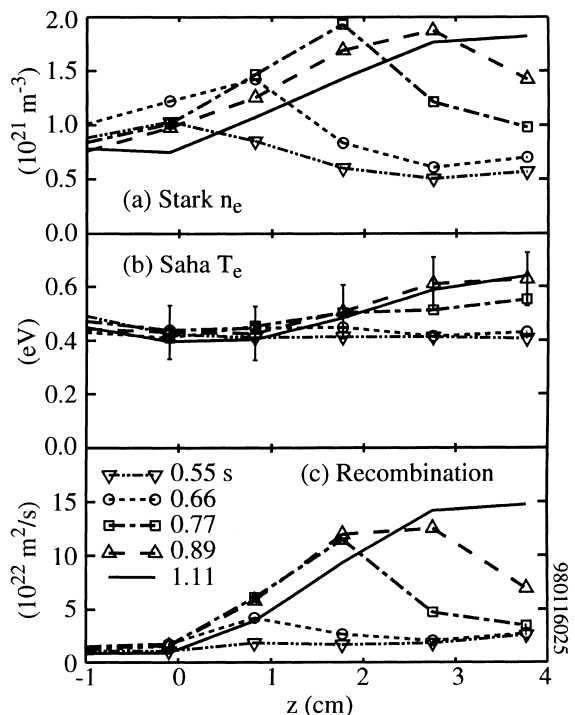


Fig. 2. Evolution of outer divertor characteristics. (a)  $n_e$  profiles derived from Stark broadening of Balmer  $8 \rightarrow 2$  line. (b)  $T_e$  derived from fit of Saha distribution to Balmer population densities ( $5 \rightarrow 8$ ). (c) Local recombination rate based on  $n_e$ ,  $T_e$ ,  $D_\gamma$  intensity, assumptions of opacity and recombinations/photon factor.

loss in the divertor, there is a high  $n_e$  (Fig. 2(a)), low  $T_e$  (Fig. 2(b)), recombining region (Fig. 2(c)) across the field of view. Because the  $T_e$  measured by probes along the divertor plate are much higher we infer that the high densities and low temperatures determined from analysis of the Balmer spectrum at this time are most likely from flux surfaces in the private flux region. As time increases, the peak density increases and the high density region expands up the plate. The  $T_e$  profile stays fairly constant. The corresponding recombination rate, determined from the  $D_\gamma$  brightnesses and the formalism discussed above, also increases and expands up the plate. The profile at the last time shown is such that a significant amount of recombination is beyond this set of spectrometer views (view O) and was primarily monitored by the view from the top of the machine (view T, Fig. 1).

In general we can follow the recombination region expansion by monitoring  $D_\gamma$  emission with a CCD camera viewing the divertor region. The images obtained in this manner are then inverted in a fashion similar to that utilized by Fenstermacher [12], to provide local emissivities. An example of such an emissivity image for the discharge of Fig. 2 is shown in Fig. 3. Early in the detachment period (Fig. 3(a), 0.7 s), the recombination is peaked below the divertor nose. This is similar to what is shown in Fig. 2(c). When the core density and detachment reach their equilibrium values, the recombination region has increased in intensity and expanded along flux surfaces (Fig. 3(c), 1.0 s). The recombination is concentrated at the outer divertor between the x-point and the plate on flux surfaces that are detached (plate plasma pressure significantly lower than upstream in the SOL). As part of the expansion of the recombination region, the edge closest to the x-point moves upward with a velocity of  $\sim 10$ – $15$  cm/s.

### 4. Relative magnitude of recombination and divertor plate ion sinks

The detailed profiles of recombination can be integrated to obtain the total recombination sink ( $I_R$ ) affecting each divertor plate. We utilize recombination ‘flux’ profiles ( $\#/m^2/s$ ) from views O and T as shown in Fig. 2. The plane of integration is assumed to be the vertical surface of the outer divertor plate for view O and a horizontal plane through the x-point for view T. Toroidal symmetry must be assumed as well. A similar integration of probe  $I_{SAT}$  over the divertor surfaces is used to determine the divertor ion sink,  $I_P$ . The total ion sink (also source) is

$$I_S = I_R + I_P. \quad (2)$$

These integrals, for the outer divertor region, are displayed in Fig. 4(a) for the same ohmic discharge of

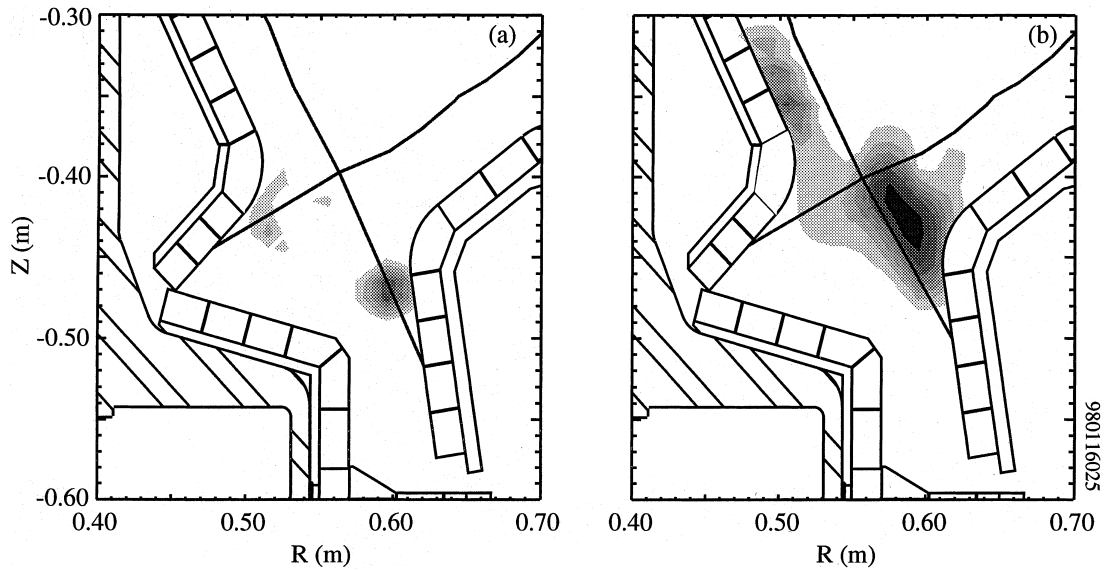


Fig. 3.  $D_\alpha$  emission pattern from inverted CCD images corresponding to the discharge shown in Fig. 2. The contour spacing is  $1 \text{ kW/m}^3$ . (a) The beginning of detachment at 0.7 s, max contour =  $5 \text{ kW/m}^3$ . (b) Detachment equilibrium at 1.0 s, max contour =  $8 \text{ kW/m}^3$ . The recombination region expansion during detachment is primarily along flux surfaces.

Figs. 2 and 3. Note that we limit the ion current integral to regions that detach (below the divertor nose) and correspond to the concentration of outer divertor recombination.  $I_p$  starts decreasing at  $\sim 0.73 \text{ s}$ , dropping to  $\sim 0.25$  of its highest value. The local drop in current can be much larger (e.g.  $\sim 10$ ). The decrease in  $I_p$  occurs later than the local changes in recombination and ion current.

Recombination does not appear to explain all of the observed loss in ion current. Substantial levels of  $I_R$  are

observed before any change in slope of  $I_p$ . In addition, the rise in the recombination sink,  $I_R$ , does not equal the drop in  $I_p$ . The total ion sink (or source),  $I_S$ , starts decreasing at 0.75 s and reaches an equilibrium value later. By the end of the shot *most ions* ( $\sim 75\%$ ) *created in the divertor recombine before reaching the plate*.

Based on a ‘two-point’ model (e.g. Ref. [13]) one might expect the total ion sink (ion source) to scale as  $n_e^2/P^{3/7}$  where  $n_e$  is the upstream density. This has been termed the ‘degree of detachment’ scaling [22]. For reference we display that scaling in Fig. 4(b) utilizing the line-averaged density,  $\bar{n}_e$  (roughly proportional to the upstream density). Note the divergence between the scaling with  $\bar{n}_e^2$  and the ion source. (The power flowing into the SOL is roughly constant.) This further emphasizes the point that recombination is not the complete reason for the drop in plate current,  $I_p$ . In addition, the ion source rate does not increase as expected. *Both a loss in ion source and an increase in the recombination sink lead to the observed drop in plate current*. The magnitude and time behavior of  $I_p$ ,  $I_R$  and  $I_S$  are similar for the inner divertor but smaller in magnitude.

There is a clear correlation between the total divertor ion source and the power flowing into the ionization region. To illustrate this effect we first examine the effect of adding auxiliary heating (ICRF) to a detached discharge, Fig. 5(a). This discharge is essentially the same as that shown in Figs. 2–4 up until the time ICRF heating is added (0.9 s). The amount of ICRF heating ( $\sim 1.5 \text{ MW}$  into the core) is similar in magnitude to the ohmic heating ( $\sim 2 \text{ MW}$ ). When the ICRF is turned on,

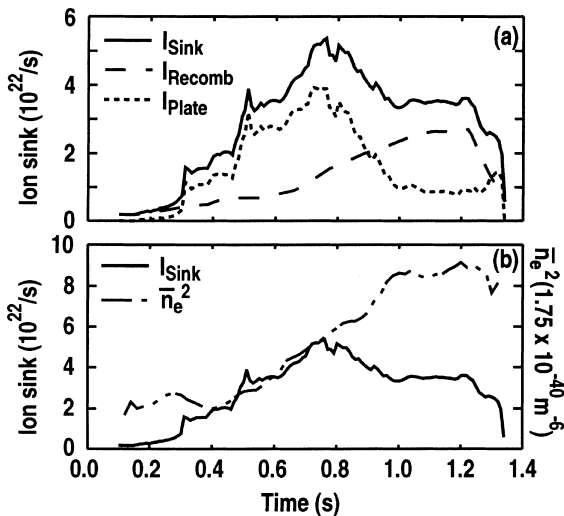


Fig. 4. (a) Ion sinks for the outer divertor plate. (b) Comparison of the outer divertor ion source to  $\bar{n}_e^2$ .

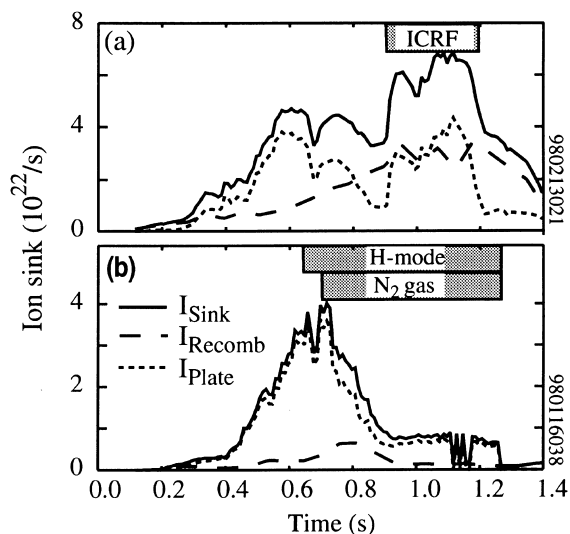


Fig. 5. Outer divertor ion sinks for (a) ICRF heating of detached plasma; and (b) detachment of an H-mode plasma with  $N_2$  gas.

the divertor is just approaching a detached divertor equilibrium. The immediate effect is for the divertor plasma to reattach over much of the plate. The current to the plate increases to values close to that measured in the ‘attached’ state. Divertor and core radiation increase by  $\sim 0.75$  MW indicating that  $\sim 0.75$  MW additional power flows into the ionization region. The concentration of recombination along the outer divertor leg moves back close to the plate but  $I_R$  decreases only slightly in magnitude! *The primary result of adding power to this detached divertor plasma was to increase the ion source.*

There are also cases where the power flowing into the ionization region decreases. We examine an H-mode discharge where the divertor is not detached through an increase in density (as in the above cases) but rather brought about by increasing impurity radiative losses through injection of  $N_2$  gas, Fig. 5(b). The ICRF heating and H-mode begin at 0.5 and 0.65 s, respectively.  $N_2$  injection commences at 0.7 s. The divertor starts to detach, with accompanying ion current loss, immediately after initiation of the  $N_2$  gas feed. The drop in ion current to the outer plate is similar to the ohmic cases discussed earlier. However, in this case the recombination sink is very low and decreasing as detachment ensues! This result emphasizes that a recombination sink is not necessary to reduce the ion current to the plates. In this case the reduction of the ion source upstream from the divertor plates is the primary cause.

The lack of recombination in these detached H-mode discharges has further implications. We can rule out recombination as a source of ion momentum loss in competition with ion-neutral collisions, at least in these

types of discharges. More generally, we have also shown that recombination is not a necessary condition for divertor detachment.

## 5. Discussion

The above results clearly show that recombination plays a varying role as a sink for ions during divertor detachment. Even in the cases where the recombination sink,  $I_R$ , is maximized, we still need to invoke a decrease in ion source rate,  $I_S$ , to explain the decrease in  $I_P$ . We believe that the limitations (and decreases) in power flow into the ionization region are the reasons for limitations (and decreases) in  $I_S$  as the core plasma density is increased. This has been previously predicted [11,23]. For the purposes of discussion we write down the power balance for the divertor (both inner and outer) in a convenient form:

$$P_{\text{SOL}} = P_{\text{RAD,D0}} + P_{\text{RAD,Z}} + P_{\text{PLATE}}, \quad (3)$$

$$\text{where } P_{\text{PLATE}} = eI_P \times (\gamma T_e + \varepsilon), \quad (4)$$

$$P_{\text{RAD,D0}} \sim eI_S \times (20\text{--}30 \text{ eV}) + eI_R \times (10\text{--}12 \text{ eV}). \quad (5)$$

$P_{\text{RAD,D0}}$  and  $P_{\text{RAD,Z}}$  are the radiated power in the divertor due to  $D^0$  and impurities, respectively,  $\varepsilon$  the ionization potential, and  $I_{P,R,S}$  has units of #/s. The first term of  $P_{\text{RAD,D0}}$  is the radiation loss from the plasma for each ionization. We have assumed that charge-exchange losses are negligible and  $T_i = T_e$ . We will assume 20 eV of energy lost per ionization. The second term of Eq. (5) is the loss of the ions’ potential energy from the plasma through volume recombination ( $eI_R \times \varepsilon$ ) as opposed to at the plate ( $eI_P \times \varepsilon$ ). We collect terms in this equation to achieve a better correspondence to measured quantities and define a new quantity  $P_{\text{IONIZ}}$ , the power that must be expended in the ionization region in order to create  $I_S$  ions/s:

$$P_{\text{SOL}} \sim eI_S \times (20 \text{ eV} + \varepsilon) + P_{\text{RAD,Z}} + eI_P \times (\gamma T_e), \quad (6)$$

$$P_{\text{IONIZ}} \equiv eI_S \times (20 \text{ eV} + \varepsilon) \sim P_{\text{SOL}} - P_{\text{RAD,Z}} - eI_P \times (\gamma T_e). \quad (7)$$

$I_S$  can be reduced by a reduction in power flowing into the SOL or by radiation from impurities in hotter regions of the divertor. This possibility is, of course, dependent on the momentum and particle balance as well. Implicit in this analysis is the assumption, based on experiment and modeling [24], that practically all of the divertor ions originate *in* the divertor.

Let us return to the discharges shown in Fig. 5 where we will be addressing the total effect on both divertors. In the first discharge (a) we find that the addition of rf power results in increases for  $P_{\text{SOL}} (\sim +1.1 \text{ MW})$ ,

$P_{\text{RAD,Z}}$  (+0.15–0.3 MW) and  $eI_p \gamma T_e$  ( $\sim +0.45$  MW based on probes). The increase in power available for ionization [Eq. (7)] should then be 0.35–0.5 MW. The corresponding change in  $P_{\text{IONIZ}}$  calculated from  $\Delta I_S$  is 0.27 MW. A similar analysis applied to the H-mode discharge of Fig. 5(b), however, now with a decrease in  $P_{\text{SOL}}$ , leads to similar conclusions. Increases or decreases in the power available for ionization can affect the divertor ion source, and thus the current to the plates.

## 6. Summary

Utilizing measurements of  $n_e$  and  $T_e$  along the same viewing chords as Balmer series line emission we are able to determine the local recombination rate as a function of position in the divertor. We find that the recombination region expands from the divertor plate towards the x-point, roughly along flux surfaces, as  $\bar{n}_e$  increases and detachment deepens. Comparing the total volumetric recombination ion sink to the plate ion current remaining during detachment, we find that volume recombination eliminates between 10% and 75% of the ion flow before it reaches the divertor plate, the lowest values are for H-mode plasmas where the detachment is induced by injection of  $\text{N}_2$  gas. Recombination is most important as an ion sink for discharges where detachment is induced through  $\text{D}_2$  gas puffing and resultant core density rise. The remaining fraction of the observed ion current loss is due to reductions in the ion sources upstream from the plate. Changes in ion source rate are consistent with changes in the power flowing from the SOL into the divertor region.

Volume recombination can be very important in determining the loss of ion current to the plates during detachment. Changes in the upstream ion source rate are equally important. These results also indicate that volume recombination is not a necessary condition for detachment (for either ion current loss or pressure loss).

## Acknowledgements

The authors wish to thank the entire Alcator group for assistance in acquiring this data. In particular we appreciate the assistance by S. Wukitch with rf power

balance and J. Goetz with radiation accounting. We would also like to thank C.S. Pitcher and P.C. Stangeby for stimulating discussions. This work was supported by the U.S. Department of Energy under contract #DE-AC02-78ET51013.

## References

- [1] G.F. Matthews, *J. Nucl. Mater.* 220–222 (1995) 104.
- [2] P.C. Stangeby, *Nucl. Fusion* 33 (1993) 1695.
- [3] C.S. Pitcher, P.C. Stangeby, *Plasma Phys. Control. Fusion* 39 (1997) 779.
- [4] B. Lipschultz, J. Goetz, B. LaBombard et al., *J. Nucl. Mater.* 220–222 (1995) 50.
- [5] S. Allen and the DIII-D Team, *Plasma Phys. Control. Fusion* 37 (1995) A191.
- [6] J. Neuhauser et al., *ibid.* A37.
- [7] A. Loarte et al., *J. Nucl. Mater.* 241–243 (1997) 118.
- [8] F. Wising et al., *Contrib. Plasma Phys.* 36 (1996) 136.
- [9] G.D. Porter et al., *Phys. Plasmas* 3 (1996) 1967.
- [10] K. Borass et al., *J. Nucl. Mater.* 241–243 (1997) 250.
- [11] S.I. Krasheninnikov et al., *Phys. Plasmas* 4 (1997) 1638.
- [12] M.E. Fenstermacher et al., *ibid.* 1761.
- [13] D. Lumma, J.L. Terry, B. Lipschultz, *ibid.* 2555.
- [14] B. Napiontek et al., Line and recombination emission in the ASDEX upgrade divertor at high density, in: *Proceedings of the 24th European Conference on Controlled Fusion and Plasma Physics*, Berchtesgarden, Germany, June 1997, Paper P4.008.
- [15] G.M. McCracken et al., *Nucl. Fusion*, 38 (1998) 619.
- [16] J.L. Terry, B. Lipschultz, A. Yu, Pigarov et al., *Phys. Plasmas* 5 (1998) 1759.
- [17] I.H. Hutchinson et al., *Phys. Plasmas* 1 (1994) 1511.
- [18] B. LaBombard et al., *Phys. Plasmas* 2 (1995) 2242.
- [19] R.D. Bengston, J.D. Tannich, P. Kepple, *Phys. Rev. A* 1 (1970) 532.
- [20] J.L. Terry, et al., these Proceedings.
- [21] J.L. Terry, B. Lipschultz, B. LaBombard, D.A. Pappas, Volume recombination in Alcator C-Mod divertor plasmas, in: *Proceedings of the 24th European Conference on Controlled Fusion and Plasma Physics*, Berchtesgarden, Germany, June 1997, Paper P2.022.
- [22] A. Loarte, R.D. Monk, J.R. Martin-Solis, *Nucl. Fusion* 38 (1998) 331.
- [23] S.I. Krasheninnikov et al., *Phys. Plasmas* 2 (1995) 2717.
- [24] M. Umansky, S.I. Krasheninnikov, B. LaBombard, J.L. Terry,
- [24] M. Umansky, S.I. Krasheninnikov, B. LaBombard, J.L. Terry, 5 (1998) 3373.